Automatic non-contact monitoring of the respiratory rate of neonates using a structured light camera

Johanna Gleichauf[1], Christine Niebler[1], and Alexander Koelpin[2]

***Abstract*— This paper introduces an automatic non-contact monitoring method for measuring the respiratory rate of neonates using a structured light camera. The current monitoring bears several issues causing pressure marks, skin irritations and eczema. A structured light camera provides distance data. Our non-contact approach detects the thorax area automatically using a plane segmentation and calculates the respiratory rate from the movement of the thorax. Our method was tested and validated using the baby simulator SimBaby by Laerdal. We used different breathing rates corresponding to preterm neonates, mature neonates and babies aged up to nine months as well as two different breathing modes with differing breathing strokes. Furthermore, measurements were taken of two positions: the baby lying on its back and on its stomach.**

I. INTRODUCTION

The current monitoring of the respiratory rate of preterm neonates on the Neonatal Intensive Care Unit (NICU) holds several issues. The measurements include the usage of electrocardiogram (ECG) electrodes (impedance pneumography), pulse oximeter, transcapnodes as well as a ventilator itself. As these methods require the direct contact with the baby's body and are cable-based, risks like pressure marks, skin irritations and eczema are possible. Furhermore, artifacts can be caused by the sweat of the child. As preterm neonates are under-developed their skin is still very sensitive. In order to minimize skin irritations and to simplify the care of the babies e.g. changing the diapers, a non-contact monitoring method shall be developed.

There are non-contact measuring methods based on infrared imaging [1–6], RGB-cameras [7–10], structured light plethysmography [11–13], RGB-D cameras [14–22] as well as radar [23–29]. Many of these approaches have only been tested on adults, require markers, are light-dependent or are not completely automated. Structured light cameras have the advantage that they are independent of lighting conditions and do not require the face to be visible as would be necessary with infrared cameras for example. There are two approaches using a structured light camera which have been tested with neonates. The first one requires two cameras and calculates the breathing volume [30, 31]. Out of the volume change the respiratory rate is estimated. This procedure is more complex than needed as calculating the volume would not be necessary for estimating the respiratory rate. Also one camera would be enough. The second approach is intended for open incubators and requires the manual selection of the measurement points, so the thorax is not detected automatically [32]. Additionaly this approach was only tested on premature babies and is specialised on this frequency range. We propose a method based on a structured light camera which automatically determines the thorax area and then measures the respiratory rate of preterms (40 - 60 breaths per minute (BPM)), mature neonates (40 - 50 BPM) and babies aged up to nine months (20 - 30 BPM) [33]. Tests were made with the baby lying in different positions such as on the back or stomach. Furthermore different depths of breaths are investigated.

[1]Johanna Gleichauf and Christine Niebler are with the Department of Electrical Engineering, Precision Engineering and Information Technology, Technische Hochschule Nuremberg Georg Simon Ohm, Nuremberg, Germany johanna.gleichauf@th-nuernberg.de

[2]Alexander Koelpin is with the Institute of High-Frequency Technology, Hamburg University of Technology, 21073 Hamburg, Germany; alexander.koelpin@tuhh.de

II. APPROACH

A. Theory

Structured light cameras send out a light pattern which is distorted if an object lies in front [39]. The distortion of the pattern can be used to calculate the distance. The change of distance of the thorax can therefore be measured with this camera. In this paper we show the feasibility to determine the number of breaths per minute automatically using a structured light camera. The following section describes the required setup and algorithms.

B. Setup

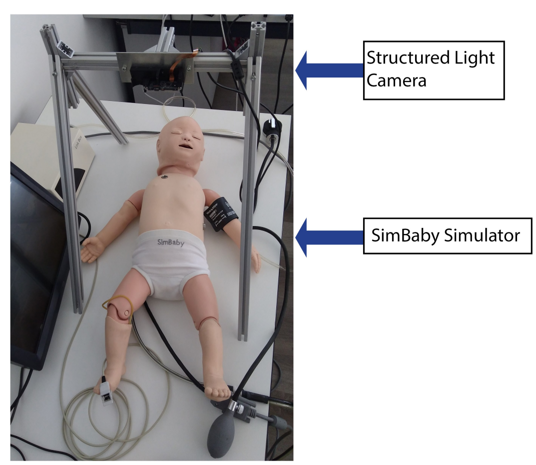

Fig. 1. Sensor setup: The camera is positioned at a distance of approximately 40 cm to the SimBaby simulator.

The camera is positioned at a distance of around 40 cm to the table which equals the proportions of a closed incubator. The SimBaby simulator by Laerdal is placed underneath the

978-1-7281-1990-8/20/$31.00 ©2020 IEEE

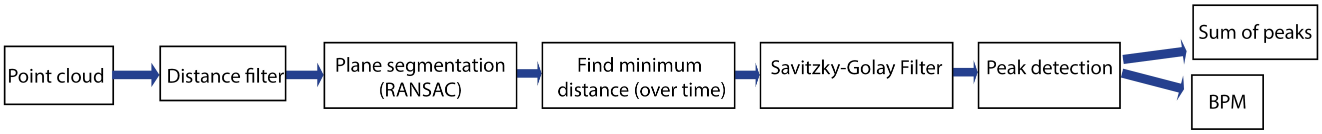

Fig. 2. Flowchart of the algorithm

camera (Fig. 1). The simulator has the size of a 9 months old baby and uses a compressor to move the thorax.

The structured light camera used is the Astra Orbecc Stereo. It has a depth resolution of 640x400 points and has a field of view of H67.9° V45.3° D78° ±3.0°. The camera delivers a temporal resolution of 30 FPS. The operating temperature lies between 10°C and 40°C and can therefore be used within an incubator. The camera is connected via USB to an Ubuntu 16.04 computer with the ROS version Kinetic installed. The camera driver used is the ROS package *ros_astra_camera*. Robot Operating System (ROS) is a middleware which allows easy communication with the camera and data processing.

C. Algorithm

Fig. 2 shows the flowchart of the used algorithm. The camera delivers point clouds. First of all, all points with a distance greater than 35 cm are removed as they would correspond to the table or bed.

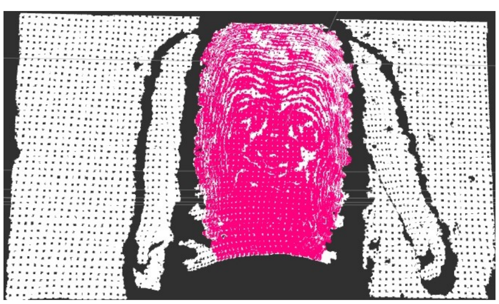

Fig. 3. Point cloud of a baby lying on its back displayed in rviz [38]. The segmented thorax plane can be seen in the middle (magenta) with the arms positioned at both sides. The white points show the rest of the point cloud (table and arms).

The next step uses a Random Sample Consensus (RANSAC) based plane segmentation from the Point Cloud Library (PCL) [34] with a distance threshold of 2 cm and the chosen model type called SACMODEL_PLANE. The threshold defines which points are part of the same plane i.e. two points with a distance of 2 cm to each other will still belong to the same plane. The segmented points are part of the thorax plane (see Fig. 3). The point with the minimal distance is automatically found and plotted over the time (example see Fig. 4). Once a dataset of 33 minimal distance values over time is available a peak detection as described in [37] is used to determine the number of breaths. Following the peak detection is applied to the next 33 values. The window size was set to this value, as there shall be a new BPM value at least every 5 s (as a hospital monitor would deliver). We get a new BPM value around every 3 s, which means around 1020 measurements per hour. The respiratory rate (RR) in BPM is calculated from the number of breaths within each window over the time in seconds:

$$RR = \frac{breaths}{time} \cdot 60 \tag{1}$$

As artifacts can occur within the signal a Savitzky-Golay filter based on Gram polynomials [35] [36] is applied to smooth the data first. The lower the breathing rate the greater effect artifacts have on the result. For this reason the filter is parametrized (polynomial order and window size for smoothing). The values depend on the mean breathing rate resulting from the first three peak detections (each window holding 33 values):

TABLE I
PARAMETERS FOR SAVITZKY-GOLAY FILTER

BPM	Window size	Polynomial order
≤ 18	11	10
18 - 50	3	2
50 - 62	3	1
> 62	None	None

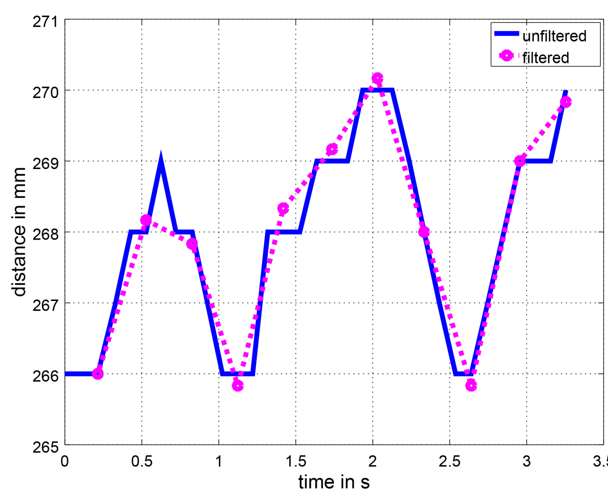

Fig. 4. Section of the respiratory signal with the baby lying on its back in *deep* mode. The set breathing rate is 50 BPM which means that the filter window size is 3 so that there are 11 filter windows in this section. Each filter window ends at the marked magenta point. Filtered signal (magenta), unfiltered signal (blue).

Fig. 4 shows a section of the respiratory signal with the baby lying on its back and breathing with a rate of around 50

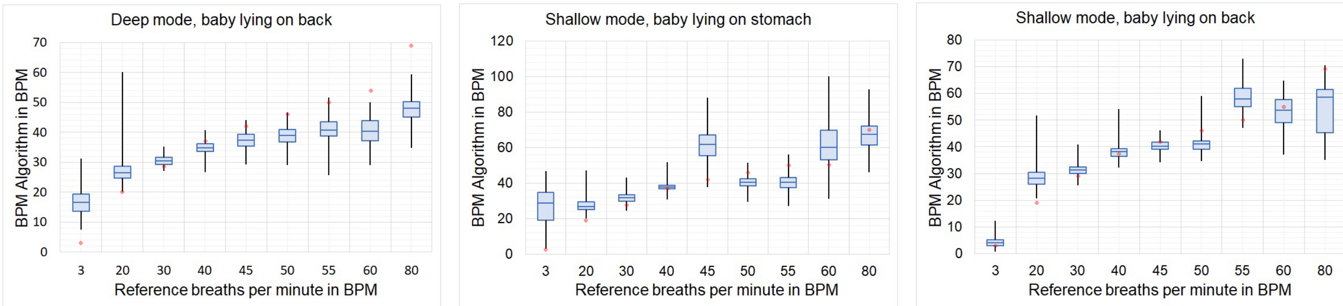

Fig. 5. Box-whisker-plot in *deep* mode lying on its back (le.) and in *shallow* mode with the baby lying on its stomach (mi.) and back (ri.). The maximum difference to the reference within the norm range is 14 BPM for *deep* mode lying on its back, 20 BPM for *shallow* mode lying on its stomach and 9 BPM for *shallow* mode lying on its back. In both modes the respiratory rate can be detected.

BPM. The blue signal is the unfiltered signal, the magenta signal the filtered one.

As the number of peaks can vary depending at which point within the data curve the window ends, a moving average window of 18 small windows (594 distance values) is used for calculating the BPM. The window is moved by the size of one dataset of 33 points.

III. RESULTS

The algorithm was tested with 36 datasets holding data recorded with different respiratory rates (3, 20, 30, 40, 45, 50, 55, 60 and 80 BPM), different breathing modes (*deep* with a stroke varying between 2 - 5 mm and *shallow* with a stroke of 1 - 3 mm. The variation depends on the frequency. With a higher frequency the stroke decreases.), as well as two positions of the baby: lying on its back or its stomach. Each dataset was run for one hour. As reference, the number of breaths for each dataset were manually counted for 15 minutes and multiplied by four to receive the number of breaths per hour. (A nurse would usually count the number of breaths only for a minute.) This showed that the set BPM does not necessarily display the actual BPM. The algorithm was used to calculate the number of breaths automatically and delivered a measurement around every 3 s. Fig. 6 shows the results for the baby lying on its stomach using *deep* mode. The box-whisker-plot is a statistical tool which displays the median, minimum, maximum and upper and lower quartiles of each dataset. The small red dots display the actual reference value. The precision is the highest for respiratory rates between 20 and 60 BPM with a maximum difference of 6 BPM. At the edge frequencies the difference rises. The lower the frequency the larger the effect of artifacts and therefore the precision is lower. If the frequency is very high some peaks might not be detected anymore. A respiratory rate of 3 BPM or 80 BPM is not within the norm range of a baby, but was tested in order to show that the trend i.e. increase or decrease of the respiratory rate can be detected. All in all it can be said that the precision is the highest in *deep* mode when the baby is lying on its stomach as the moved plane is bigger and will therefor deliver more stable measurements. The window size also influences the precision, depending where the signal is cut.

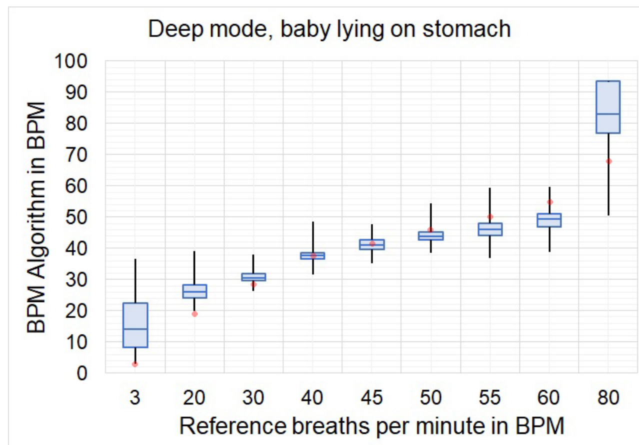

Fig. 6. Box-whisker-plot in *deep* mode. The baby is lying on its stomach. The maximum difference to the reference within the norm range is 6 BPM.

IV. CONCLUSIONS

In this paper we presented a fully automated non-contact method for measuring the respiratory rate of neonates based on a structured light camera. We validated our method with 36 datasets of different rates, positions of the baby as well as different breathing modes. As expected the precision is the highest when the baby is lying on its stomach and having a breathing stroke of 2 mm to 5 mm. As we are covering so many different breathing rates the data processing is more complex as the filtering depends on each frequency. In the future we intend to increase the precision by making the filter algorithm adaptive to the given frequency. In order to increase the robustness, the system could be extended by other measuring methods. Furthermore this approach will be tested with real babies within a NICU. We are currently working on the ethical approval proposal for our planned study.

ACKNOWLEDGMENT

This work was funded by the Federal Ministry of Education and Research (BMBF). Funding reference: 13FH546IX6

Johanna Gleichauf thanks AGNF (Arbeitsgemeinschaft für Notfallmedizin in Fürth) for lending the SimBaby.

REFERENCES

[1] A. K. Abbas et al. "Neonatal non-contact respiratory monitoring based on real-time infrared thermography". In: *BioMedical Engineering OnLine 5.4 (2011), pp. 1124-35* (2011).

[2] A. K. Abbas and S. Leonhard. "Intelligent neonatal monitoring based on a virtual thermal sensor". In: *BMC Medical Imaging 14.1* (2014).

[3] S. L. Bennett, R. Goubran, and F. Knoefel. "The detection of breathing behavior using Eulerian-enhanced thermal video". In: *Proceedings of the Annual International Conference of the IEEE Engineering in Medicine and Biology Society, EMBS 2015-November, pp. 7474-7477* (2015).

[4] J. H. Klaessens et al. "Development of a baby friendly non-contact method for measuring vital signs: First results of clinical measurements in an open incubator at a neonatal intensive care unit". In: *8935 (2014), 89351P* (2014). DOI: aspx?doi=10.1117/12.2038353. URL: http://proceedings.spiedigitallibrary.org/proceeding.

[5] C. B. Pereira et al. "Estimation of respiratory rate from thermal videos of preterm infants". In: *Proceedings of the Annual International Conference of the IEEE Engineering in Medicine and Biology Society, EMBS (2017), pp. 3818 - 3821* (2017).

[6] S. Xu et al. "Neonatal non-contact respiratory monitoring based on real-time infrared thermography". In: *BioMedical Engineering OnLine 5.4 (2014), pp. 1124-35* (2014). URL: http://www.biomedicalengineering-online.com/content/10/1/93%7B%5C%%7D5C%7B%5C%%7D5Cnhttp://www.pubmedcentral.nih.gov/articlerender.fcgi?artid=3985994%7B5C&%7Dtool=pmcentrez%7B%5C&%7Drendertype=abstract.

[7] S. Davis et al. "Continuous non-contact vital sign monitoring in neonatal intensive care unit". In: *Healthcare Technology Letters 1.3 (2014), pp. 87-91* (2014). URL: http://digital-library.theiet.org/content/journals/10.1049/htl.2014.0077.

[8] L. Tarassenko et al. "Noncontact video-based vital sign monitoring using ambient light and auto-regressive models". In: *Physiological Measurement 35.5 (2014), pp. 807-831* (2014).

[9] A. Al-Naji and J. Chahl. "Remote respiratory monitoring system based on developing motion magnification technique". In: *Biomedical Signal Processing and Control 29 (2016), pp. 1-10* (2016). URL: http://dx.doi.org/10.1016/j.bspc.2016.05.002.

[10] M. A. Hassan et al. "Novel health monitoring method using an RGB camera". In: *Biomedical Optics Express 8.11 (2017), p. 4838* (2017). URL: http://dx.doi.org/10.1364/BOE.8.004838.

[11] E. Lauhkonen, B. G. Cooper, and R. Iles. "Mini review shows that structured light plethysmography provides a non-contact method for evaluating breathing patterns in children". In: *Acta Paediatrica, International Journal of Paediatrics (2019), pp. 1398?1405* (2019).

[12] M. Ghezzi et al. "Structured Light Plethysmography (SLP): Management and follow up of a paediatric patient with pneumonia". In: *Respiratory Medicine Case Reports 22 (2017), pp. 67-69* (2017). URL: https://doi.org/10.1016/j.rmcr.2017.06.004.

[13] H. Hmeidi et al. "Tidal breathing parameters measured by structured light plethysmography in children aged 2-12 years recovering from acute asthma/wheeze compared with healthy children". In: *Physiological Reports 6.12 (2018), pp. 1-13* (2018).

[14] J. Penne et al. "Robust real-time 3D respiratory motion detection using time-of-flight cameras". In: *(2009), pp. 8-9* (2009).

[15] M. Martinez and R. Stiefelhagen. "Breathing rate monitoring during sleep from a depth camera under real-life conditions". In: *2017 IEEE Winter Conference on Applications of Computer Vision, WACV 2017. pp. 1168 - 1176* (2017).

[16] A. Procházka et al. "Microsoft Kinect visual and depth sensors for breathing and heart rate analysis". In: *Sensors (Switzerland). pp. 1 - 11* (2016).

[17] U. Wijenayake and S. Y. Park. "Real-time external respiratory motion measuring technique using an RGB-D camera and principal component analysis". In: *Sensors (Switzerland)* (2017).

[18] N. Bernacchia et al. "Non contact measurement of heart and respiration rates based on Kinect". In: *2014 IEEE International Symposium on Medical Measurements and Applications (MeMeA)* (2014).

[19] S. Rihana et al. "Kinect2 - Respiratory movement detection study". In: *2016 38th Annual International Conference of the IEEE Engineering in Medicine and Biology Society (EMBC)* (2016).

[20] F. Benetazzo et al. "Respiratory rate detection algorithm based on RGB-D camera: theoretical background and experimental results". In: *Healthcare Technology Letters (Volume: 1 , Issue: 3 , 09 2014)* (2014).

[21] P. Nguyen et al. "WiKiSpiro: Non-contact Respiration Volume Monitoring during Sleep". In: *S3 Proceedings of the Eighth Wireless of the Students, by the Students, and for the Students Workshop. pp. 27-29* (2016).

[22] A. Procházka et al. "Breathing Analysis Using Thermal and Depth Imaging Camera Video Records". In: *Sensors (Basel)* (2017).

[23] K. Shi et al. "A contactless system for continuous vital sign monitoring in palliative and intensive care". In: *12th Annual IEEE International Systems Conference, SysCon 2018 - Proceedings (2018), pp. 1-8* (2018).

[24] G. Vinci et al. "Six-Port Radar Sensor for Remote Respiration Rate and Heartbeat Vital-Sign Monitoring". In: *IEEE Transactions on Microwave Theory and Techniques 61.5 (May 2013), pp. 2093-2100* (2013).

[25] S. Wang et al. "A novel ultra-wideband 80 GHz FMCW radar system for contactless monitoring of vital signs". In: *2015 37th Annual International Conference of the IEEE Engineering in Medicine and Biology Society (EMBC) , Milan* (2015).

[26] G. Matthews, B. Sudduth, and M. Burrow. "A non-contact vital signs monitor". In: *Crit Rev Biomed Eng.* (2000).

[27] C. Li et al. "Radar remote monitoring of vital signs". In: *IEEE Microwave Magazine (Volume: 10, Issue: 1), pp. 47-56* (2009).

[28] Y. Yan et al. "Verification of a Non-Contact Vital Sign Monitoring System Using an Infant Simulator". In: *31st Annual International Conference of the IEEE EMBS, Minneapolis, Minnesota, USA* (2009).

[29] A. Droitcour et al. "Non-contact respiratory rate measurement validation for hospitalized patients". In: *Conf Proc IEEE Eng Med Biol Soc.* (2009).

[30] H. Rehouma et al. "A Computer Vision Method for Respiratory Monitoring in Intensive Care Environment Using RGB-D Cameras". In: *2017 Seventh International Conference on Image Processing Theory, Tools and Applications (PTA)* (2017).

[31] H. Rehouma et al. "3D imaging system for respiratory monitoring in pediatric intensive care environment". In: *Comput Med Imaging Graph* (2018).

[32] A. Cenci et al. "Non-contact monitoring of preterm infants using rgb-d camera". In: *Proceedings of the ASME 2015 International Design Engineering Technical Conferences Computers and Information in Engineering Conference* (2015).

[33] S. Bittmann. *Checklisten Paediatrie und Neonatologie*. Elsevier GmbH, 2010.

[34] *Plane model segmentation*. Accessed: 26.10.2019. URL: http://www.pointclouds.org/documentation/%20tutorials/planar%7B%5C_%7Dsegmentation.php.

[35] P. A. Gorry. "General least-squares smoothing and differentiation by the convolution (Savitzky-Golay) method". In: *Anal. Chem.1990626570-573* (1990). URL: https://doi.org/10.1021/ac00205a007.

[36] *C++ Implementation of Savitzky-Golay filtering based on Gram polynomials*. Accessed: 26.10.2019. URL: https://github.com/arntanguy/gram%7B%5C_%7Dsavitzky%7B%5C_%7Dgolay.

[37] *Find-peaks*. Accessed: 26.10.2019. URL: https://github.com/claydergc/find-peaks.

[38] *rviz*. Accessed: 13.11.2019. URL: http://wiki.ros.org/rviz.

[39] J.-F. Emmrich. *What is Structured-Light Scanning?* Accessed: 13.11.2019. URL: https://blog.medit.com/medit/what-is-structured-light-scanning.